STUDIA UBB CHEMIA, LXIV, 2,Tom I, 2019 (p. 159-174)
(RECOMMENDED CITATION)
DOI:10.24193/subbchem.2019.2.13

***Dedicated to Professor Florin Dan Irimie on the Occasion of His 65th Anniversary***

# METABOLIC ENGINEERING OF *E. COLI*: INFLUENCE OF GENE DELETIONS AND HETEROLOGOUS GENES ON PHYSIOLOGICAL TRAITS

**RÉKA SINKLER[a], MÁRTA BOTH-FODOR[a], EMŐKE ANTAL[a], HUNOR BARTOS[b], SZABOLCS LÁNYI[c], ILDIKÓ MIKLÓSSY[c*]**

**ABSTRACT.** 1,4-butanediol (BDO) is an important commodity molecule that is used as a platform chemical for the production of polybutylene terephthalate (PBT), elastic fibres (Spandex) and other materials. The homologous enzyme of *E. coli*, *succinyl-CoA synthetase* (*sucCD*) and the heterologous *malonyl-CoA reductase* from *Chloroflexus aurantiacus* (*mcr*) are key enzymes in a heterologous pathway leading to BDO production, which were introduced into a genome-engineered *E. coli* MG1655(DE3) Δ*ldhA*, Δ*pflB* strain. Knowing that the expression of recombinant proteins and gene deletions can significantly influence cellular viability, the present study was carried out to investigate the impact of the two key enzyme expression on deletion strains, helping us to analyze the physiological changes of *E. coli* strains and providing directions for further optimizations in order to achieve satisfying target product yields.

***Keywords:*** *1,4-butanediol, heterologous enzyme, Escherichia coli, metabolic engineering*

[a] *Politehnica University of Bucharest, Faculty of Applied Chemistry and Materials Science, 1-7 Gheorghe Polizu str., RO-011061, Bucharest, Romania*
[b] *University of Pécs, Faculty of Natural Sciences, Doctoral School of Chemistry, 6 Ifjúság str., Hu-7624, Pécs, Hungary*
[c] *Sapientia Hungarian University of Transylvania, Faculty of Economics, Socio-Human Science and Engineering, Department of Bioengineering, 1 Libertatii sqr., RO-530104, Miercurea Ciuc, Romania*
** Corresponding author: miklossyildiko@uni.sapientia.ro*

## INTRODUCTION

Over the last decade, the necessity of alternative bio-based processes for currently petro chemistry-derived bulk chemicals demand has emerged [1,2]. The global production of BDO is currently manufactured almost entirely from petroleum-based, non-renewable feedstock such as acetylene, butane or butadiene resulting in 1,4-butanediol (BDO) to became listed on the NICNAS High Volume Industrial Chemicals List (HVICL) [3]. A native BDO pathway does not exist in any known organism, therefore developing a bio-based production system for 1,4-butanediol (BDO) through metabolic engineering methods, utilizing *E. coli* MG1655 as host strain is considered a good alternative to classical syntheses. However, to achieve a high yield of BDO with genetic engineering tools some technical challenges have to be met, mainly concerning the metabolic performance of host cells [4-10]. In metabolic engineering projects, altering the cellular metabolism with increased substrate uptake, reduction of carbon flux leading to undesirable by-products or the extracellular export of the target product may occur in order to shift the equilibrium towards product formation [11]. These modifications and additionally, the expression of heterologous proteins/enzymes can inflict a significant metabolic burden that can lead to decrease in biomass yield and cellular viability [10].

Carneiro et. al. discusses about several physiological stresses affecting bacterial strains during recombinant protein production, while the over-expression of heterologous proteins provokes a reduction in the synthesis of biomass-related proteins, due to the unequal competition for the translation apparatus by the mRNA species synthesized from the high-level expression of recombinant material. This can be explained by different amino acid composition of the recombinant protein relative to the average composition of biomass related proteins, which causes increased metabolic imbalance in the host cells [10].

Moreover, heterologous expression of even non-toxic proteins under strong promoter control (e.g. T7) causes competition for ribosomes from the exogenous mRNAs and decreases free ribosome concentration, which can lead to cell death. Moderate overexpression can affect the cellular environment by modifying the redox equilibrium, potentially resulting in growth inhibition, toxic accumulation of acetate, reduction of carbon flux via the oxidative branch of the pentose phosphate pathway, reduced expression of housekeeping genes, and inducing of various stress responses [12]. For example, overexpressing membrane proteins can decrease cellular fitness, presumably by saturating the protein translocation system and reducing respiratory chain complex formation, which eventually leads to respiratory stress [12].

There are phenomenological, empirical models describing linear correlations between growth rate and RNA/protein ratio, and predicting an overall linear effect on protein overproduction on cellular fitness [13]. Alternatively, it has been shown by modeling supported by wet experiment data that a strongly nonlinear fitness landscape associates with the *lac* pathway of *E. coli* depending on protein yield and activity [13].

Regardless, consequences of cellular stress on population dynamics at macro and molecular levels are not well understood. The picture is even less clear in cases, where the heterologously introduced gene products require ATP or/and make use of the host redox coenzymes or they interact with the host core metabolism [12]. This is the case in our present work, where we investigate the effect of an overexpressed two-step biosynthetic pathway requiring NADH, on a genome-edited deletion mutant *E. coli* strain.

In 2011 Yim et al. reported for the first time de novo biosynthesis of 1,4-BDO via a biological platform, which constituted the base for the bio-manufacturing of 1,4-butanediol, established by Genomatica [14]. Our aim was to build a simpler biosynthetic pathway of BDO in *E. coli*, able to use and convert renewable feedstock such as glucose and glycerol. As a by-product of biodiesel industry, glycerol is considered a very attractive carbon source [15-17]. To our knowledge, our group is the first to consider glycerol as a sustainable substrate for BDO production.

In our previous work [18], we reported construction of an *E. coli* strain with knocked-out genes for ethanol, lactate and formate production (Δ*adhE,* Δ*ldhA* and Δ*pflB*), able to produce a limited quantity of 1,4-BDO (.89 mg/L BDO under microaerobic conditions and .82 mg/L under anaerobic conditions), using glycerol as carbon source [18].

Here we present physiological assessment of a designed alternative biosynthetic pathway, using a different enzyme combination leading to the target product. The pathway contains the two-subunit native enzyme of *E. coli*, succinyl-CoA synthetase (sucCD) and the heterologous malonyl-CoA reductase from *Chloroflexus aurantiacus* (mcr) under the control of a strong T7 promoter, introduced and expressed in a genome-engineered MG1655(DE3) ΔldhA, ΔpflB strain.

## RESULTS AND DISCUSSION

Given that genetic modifications, in our case gene inactivation and expression of recombinant proteins can significantly influence cellular viability, our present study tackled to investigate how expression of the two key enzymes impact cellular fitness and population stability of deletion strains, helping us to analyze physiological changes of *E. coli* strains and providing directions for further optimizations in order to achieve robust cultures with satisfying target product yields.

In the first phase of our study selection of putative enzymes (*mcr* EC 1.2.1.75 and *sucCD* EC 6.2.1.5) to our alternative heterologous pathway was carried out based on relevant literature. We considered the less studied *Chloroflexus aurantiacus* hydroxipropanoate cycle enzyme as extremely interesting due to its double specificity, with high potential also in other biosynthetic pathways.

1,4-butanediol production strains were obtained by model-driven metabolic optimization of the *E. coli* MG1655 host strain, identification of target genes for deletions was performed by metabolic flux balance analysis. The metabolic optimization was achieved by deletion of key genes *(ΔldhA* and *ΔpflB)* of the metabolic routes being competitive with the new heterologous pathway. Gene deletions were carried out using the λ-Red recombination method [19]. Expression of BDO-pathway enzymes under the control of T7 promoter was achieved after (DE3) lysogenization of the knocked-out strains. The vectors were checked by sequencing and their functionality tested by chemical transformation into the metabolically optimized strains [20]. Protein production of the strains was investigated in comparation with a specialized protein production strain. Strain optimizations were followed by examination of culture conditions of the optimized and the heterologous strains under anaerobic (oxygen-restricted) conditions. For carbon source glucose and glycerol was used providing an insight into the glycerol-utilization potential of these strains.

**Pathway design.** Heterologous reactions for 1,4-butanediol formation were selected based on literature sources and specific databases (KEGG; ECOCYC; BRENDA; PDB; NCBI). Thereafter we analyzed the key enzymatic parameters like substrate specificity, $k_{cat}$, molecular weight, subunits and genetic properties (GC content, phylogenetic distance from the host) as well. The new biosynthetic pathway employs the 4-carbon TCA cycle intermediate *succinyl-CoA*, which, in three enzymatic reduction/CoA activation steps is converted into 1,4-butanediol (Fig.1).

The designed biochemical pathway leading to BDO production is starting from succinyl-CoA, which can be converted into 4-hydroxybutyrate by a heterologous enzyme, *malonyl-CoA reductase* from *Chloroflexus aurantiacus* (*mcr*). The carboxylic group of 4-hydroxybutyrate can be activated by the native enzyme of *E. coli*, *succinyl-CoA synthetase* (*sucCD*) and in the final step the 4-hidroxybutyryl-CoA will be converted to 1,4-butanediol by the *malonyl-CoA reductase* from *Chloroflexus aurantiacus* (*mcr*).

The constraint-based models work well in the design of strains for the improved production of chemicals that belong to the central carbon metabolism, but the recombinant processes are far more complex, since the expression of recombinant proteins is generally plasmid-based, meaning that

the interaction with the central carbon metabolism is not straightforward to understand and to model. The combination of dynamic and stoichiometric models can be useful for the simulation of cell growth and metabolite and/or product formation [10].

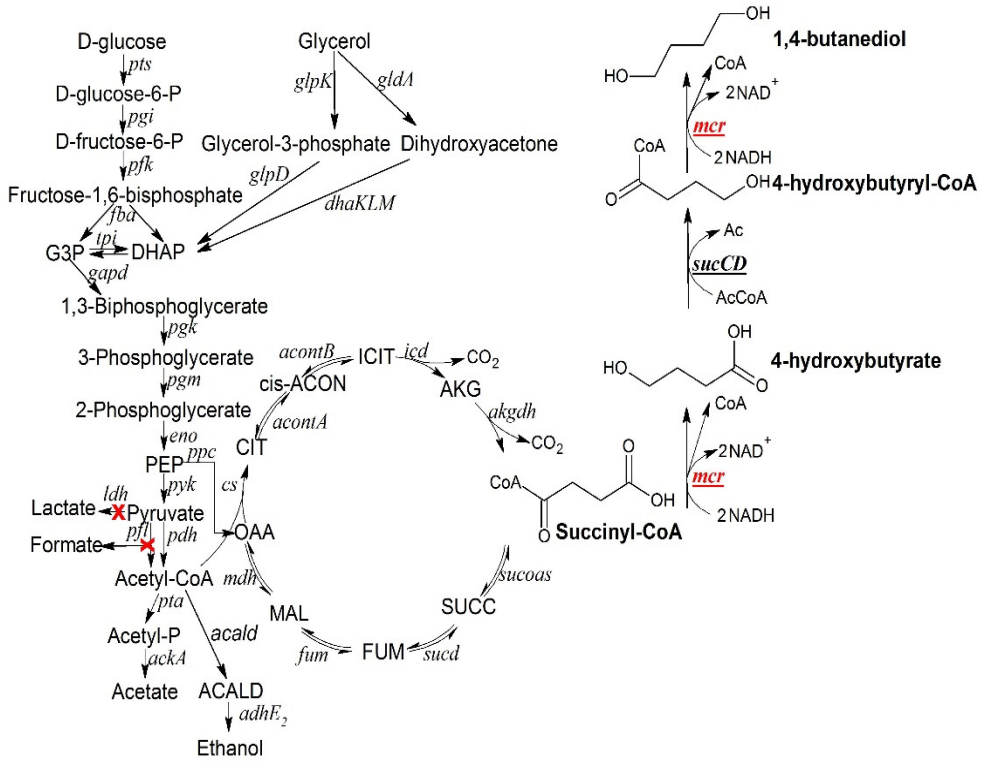


**Fig. 1.** Proposed biosynthesis pathway for 1,4-butanediol formation

Significant carbon metabolism pathways with relevant reactions of *E. coli* are depicted, the proposed BDO pathway starting from the TCA intermediate succinyl- CoA. Genetic modifications of the strain are marked in red, overexpressed endogenous ***sucCD*** gene is marked in bold letters. The image was created in ChemSketch

**Plasmid construction.** As the designed biosynthetic pathway requires the presence of two or more parallel heterologous enzymes, we decided to use the pETDuet system capable for the simultaneous expression of two genes with a strong promoter. Based on the literature these expression plasmids are currently applied successfully in several metabolic engineering applications for example butanol [21] acetoin, 2,3-butanediol [22, 23] and 3-hydroxypropionic acid biosynthesis [24].

For gene amplifications, the conventional PCR-directed molecular cloning methods were used with gene-specific primers, resulting in vectors used for protein production experiments (pGS2) and vectors, which contain two heterologously expressed genes of the BDO-production pathway (pGS2.1).

On the below gel electrophoresis images, we were able to detect the expected gene-specific PCR products as shown in Fig. 2, panel A, and the correct assembly of (pGS2) plasmid, examined by restriction digestion, and separated on a 1% agarose gel (panel B).

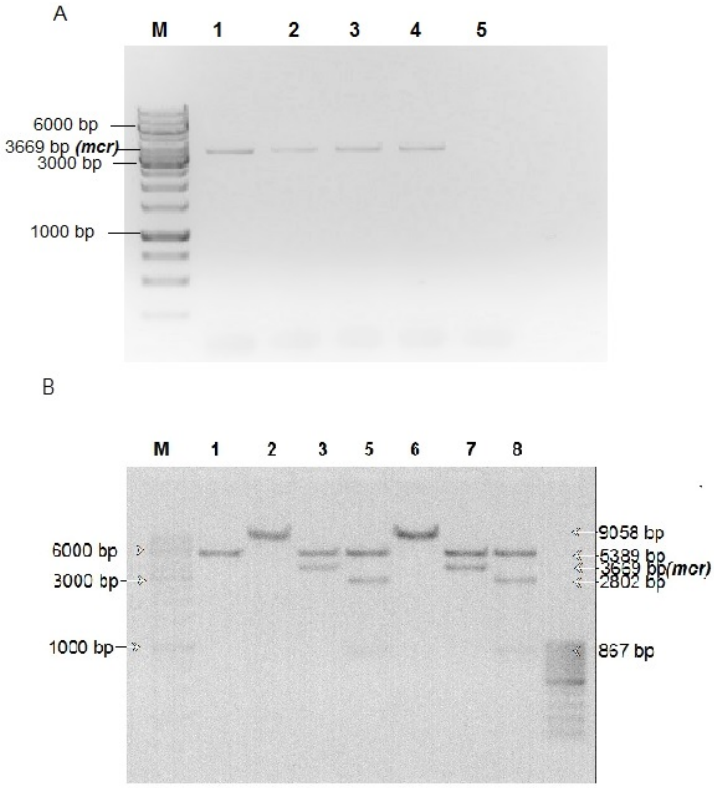


**Fig. 2.** PCR reaction products for isolation of *mcr* (A) and restriction verification of the pGS2 construct (B)

(Panel A: M- Molecular weight marker GeneRuler 1kb Thermo, Lanes: 1-5: PCR products of cloning reactions for *mcr*, the 3669 bp band corresponds to the *mcr* coding sequence, 6: no template control

Panel B: M- Molecular weight marker GeneRuler 1kb Thermo, Lanes: 1- Non-digested pGS2 vector; 2- pGS2 vector digested with *EcoRI*; 3-7: pGS2 digested with *EcoRI* and *HindIII* enzymes, the 3669 bp band corresponds to the *mcr* gene, 5,6,7,8-digestion of pGS2 with *EcoRI*, *SalI* and *HindIII* restriction enzymes, with the expected DNA fragment sizes).

*In silico* design of the vectors was carried out by the trial version of Snapgene. The restriction map of the pETDuet1-mcr-sucCD (pGS2.1) co-expression plasmid, presenting the main features is shown in Fig. 3.

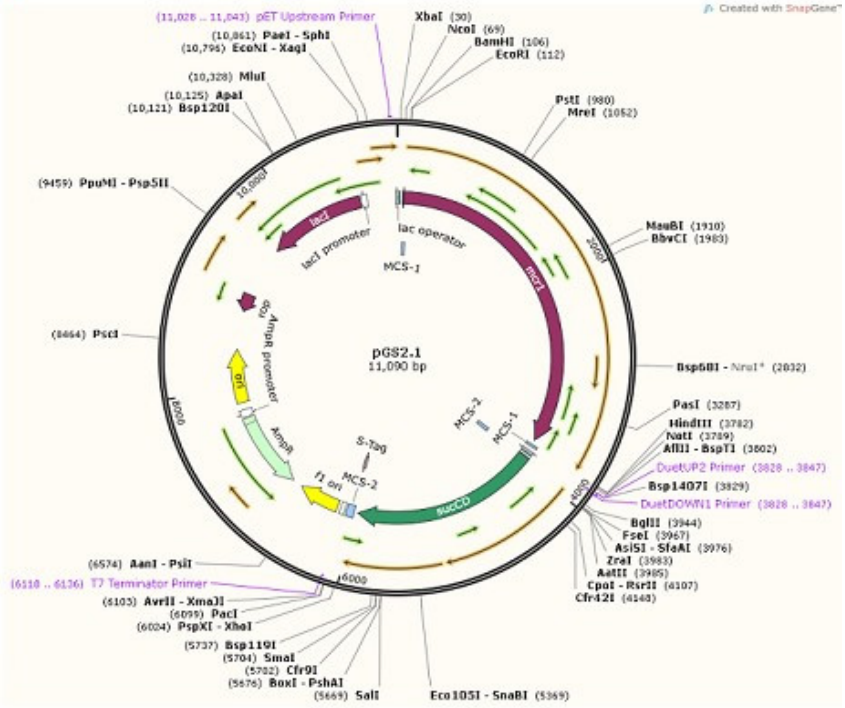


**Fig. 3.** *In silico* design of pGS2.1 vector containing the heterologous enzymes for 1,4-butanediol pathway

**Genome engineering.** To delete the key genes of metabolic routes competitive with the new heterologous pathway chromosomal gene deletions were carried out using the λ-Red recombination system [19]. Blocking off the competing metabolic pathways with the integrated biosynthetic pathway is one of the promising strategies for optimizing the yield of the target product. Redirection of the carbon flux to the BDO biosynthesis firstly was analyzed by OptKnock algorithm, after which we identified *ldhA* gene deletion to inhibit lactic acid production and deletion of the *pflB* gene for suppression of formic acid production in our previous work. Verification of genomic regions for *pflB* and *ldhA* of the wild-type MG1655(DE3) and double mutant MG14D2(DE3) was carried out by gene-specific PCR, whereas products separated on 1% agarose gel are shown in Fig. 4.

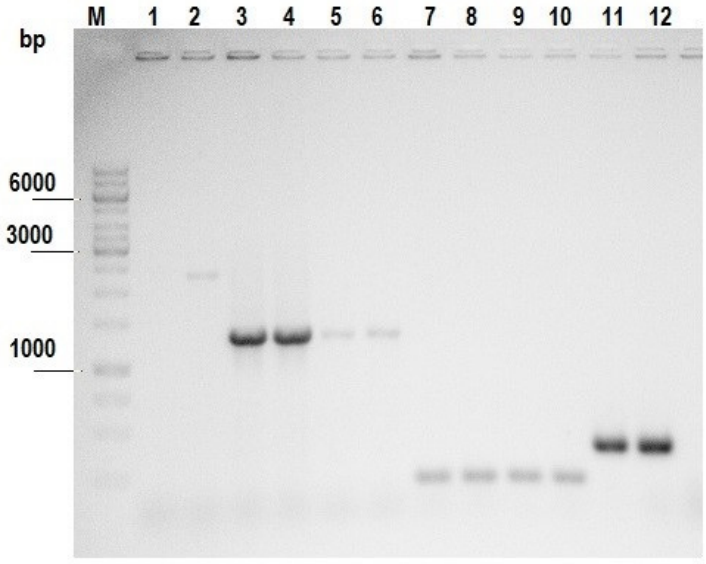


**Fig. 4.** Genotype analysis of wild-type and mutant *E.coli* strains with *pflB* and *ldhA* specific primers in PCR reactions.

(M: Molecular Weight Marker GeneRuler 1kb (Thermo); 2: *pflB* region of MG1655(DE3); 3.4: *ldhA* region of MG1655(DE3); 5.6: *ldhA* region of MG14D1(DE3), 7-9: *pflB* region of MG14D1(DE3), MG14D2(DE3) strains, 11: *ldhA* region of MG14D2(DE3) strain.) PCR products were separated by 1% AGE and visualized by RedSafe (Chembio).

**Heterologous expression**. In order to define protein production potential correlated to genomic modifications, mcr protein expression of the wild-type and double mutant strains was monitored in comparison to a specialized protein production strain. The target protein (*mcr*) expression was investigated in MG1655(DE3), MG14D2(DE3) and *Escherichia coli* BL21 Star (DE3), where chemically competent mutant strains were transformed by heat-shock with co-expression vector pGS2. Expression was induced by isopropyl β-D-1-thio-galacto-pyranoside (IPTG) in a final concentration of 0.5 mM and the cultures were maintained for 3h. Protein production was monitored after 0, 1, 2 and 3 hours of expression, by electrophoresis performed under denaturing conditions starting from samples with equal biomass ($OD_{595}$ values) of expression cultures.

Based on the results presented in the gel electrophoresis image (Fig. 5), the apparent size of the protein produced by all the studied different strains was around 130 kDa. This value agrees well with the theoretical molecular weight of *mcr,* calculated at 131.978 kDa.

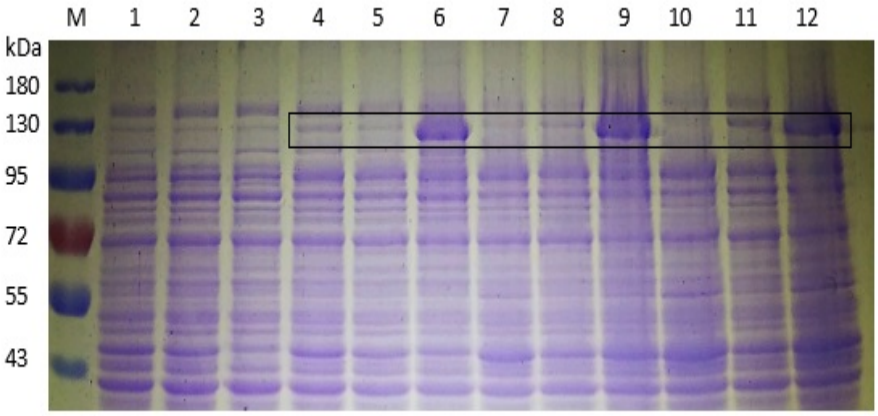


**Fig. 5.** Heterologous expression of the *mcr* enzyme in different *E. coli* strains. (M: PageRuler™ Prestained Protein Ladder, 10 to 180 kDa (Thermo); 1: MG1655(DE3)pGS2 before induction; 2. MG14D2(DE3)pGS2 before induction; 3: *E.Coli* BL21 Star (DE3)pGS2 before induction; 4,7,10: MG1655(DE3)pGS2 after 1,2 and 3 hours of induction; 5,8,11: MG14D2(DE3)pGS2 after 1,2 and 3 hours of induction; 6,9,12: *E.Coli* BL21 Star (DE3) after 1,2 and 3 hours of induction. Cellular proteins were separated by tris-glycine SDS-PAGE and stained by Commassie.

In case of pGS2-transformed, wild type MG1655(DE3) strain, protein production is less significant in all three sampling time-points, and based on the gel image, we can observe even a higher quantity of heterologous protein after the 1st hour of expression compared to samples after two and three hours of expression, respectively. In case of the double mutant strain, a slightly elevated protein production was registered in all three samples (Fig. 5, lanes 5,8,11), and a small increase in protein quantity over the time course of expression can be noted, based on the intensity of the specific protein bands.

The highest yield of produced heterologous protein was observed, as anticipated, in case of *E. coli* BL21 Star (DE3), in which case after just one hour of induction a notable quantity of *mcr* appeared, increasing with the time of expression, based on protein band intensity (Fig. 5, lanes 6,9,12).

However, in case of a similar experimental setup, studying expression of a smaller molecular weight protein of around 94 kDa (*adhE* from *Clostridium acetobutylicum*), even a triple deletion mutant strain showed comparable levels of protein expression to the same specialized *E. coli* strain (data not shown). Based on these results, we can hypothesize, that heterologous protein size has a significant influence over expression levels in non-specialized *E. coli* strains, especially if these strains harbor genomic modifications as well.

Furthermore, amino-acid composition, and presumably, phylogenetic distance of the source organism for non-codon-optimized heterologous coding sequences can be taken into account in order to further investigate and clarify this question.

**Growth dynamics investigation.** Population dynamics studies were carried out by comparing the optimized MG14D2 (DE3) strain, the production strain MG14D2(DE3)pGS2.1, as well as the MG1655(DE3) and MG14D2(DE3)pC control strains under oxygen-limited conditions in terms of maximal OD values, growth rates and phases of bacterial dynamics. In small-scale experiments, minimal media was inoculated in triplicates to an initial $OD_{595}$ of 0.1 with genetically homogeneous inoculum of the above strains, containing as carbon source glucose or glycerol at 5 g/L concentration and cultivated for 12 hours. Growth curves were compiled based on blank-corrected $OD_{595}$ values, and the data comparing the four studied strains in case of glucose and glycerol substrates, respectively, are presented in Figure 6.

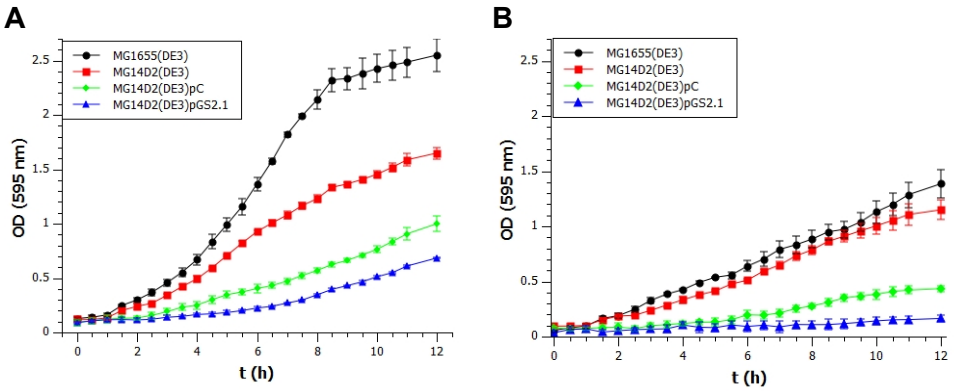


**Fig. 6.** Growth dynamics profile of the investigated strains using as sole carbon source glucose (panel A) and glycerol (panel B).

Analysis of the data presented above shows that, using glucose as carbon source, the duration of the exponential growth stage for MG1655(DE3), the lysogenized wild-type strain reached around 5 hours, while the estimated growth rate was ~0.26/h with a generation time of 2.6 hours. The recorded $OD_{595}$ values depict a standard growth dynamics profile, where individual phases can be clearly separated.

In turn, for the knock-out mutant MG14D2(DE3), a higher 3.2 hour generation time was calculated, whereas presence of an even empty plasmid required a 3.5 hour generation time for population maintenance, in case of MG14D2(DE3)pC. The generation time reflects pretty fairly, in our view

the metabolic burden of several genetic modifications, as in case of MG14D2(DE3)pGS2.1, a double mutant harboring two plasmid-borne overexpressed genes, the generation time reaches 4.1 hours, by 1.5 hours longer than in case of the initial, wild-type strain. These differences should be significant especially from the point of view of process engineering. The calculated generation times reflect the maximal optical density values reached by each strain, as well as the growth dynamics.

In similar fashion, in case of using glycerol as the sole carbon source an elongated growth dynamic profile can be distinguished in case of all four strains. The strain MG14D2(DE3)pC containing the empty plasmid was hardly able to adapt to the culture conditions in the studied timeframe, the estimated growth rate being only ~0.15/h. In comparison, the double deletion mutant MG14D2(DE3) showed a ~ 0.23/h value with a generation time of 2.79 hours, comparable to that of the wild-type strain.

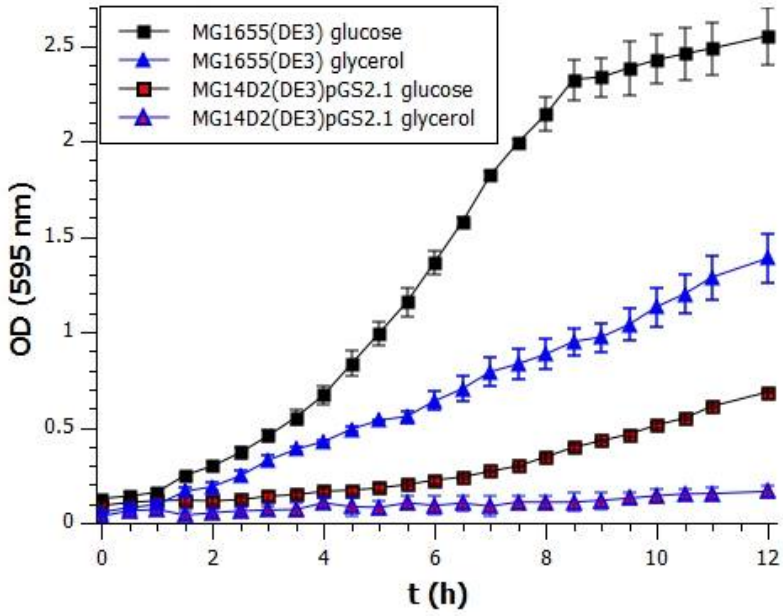


**Fig. 7.** Comparison of growth dynamics of the control MG1655(DE3) and the production strain MG14D2(DE3)pGS2.1 using glucose or glycerol as carbon source

Comparing the control MG1655(DE3) to the double mutant and heterologous enzyme (*mcr, sucCD*) expressing MG14D2(DE3)pGS2.1 strains, a significant difference in the population growth dynamics can be observed. According to the results shown in figure 7, even in conditions of highly

assimilated glucose carbon source, genetic interventions greatly influence growth profiles, cause a significant decrease in biomass production due to competition for cellular resources and create a prolonged generation time in order for the cells to function in altered intracellular metabolic environment. Nevertheless, in order to approach the theoretical growth rate (0.59/h) obtained during *in silico* simulations, further long-term adaptation experiments are foreseen in order to investigate adaptability and robustness of these *E. coli* strains.

## CONCLUSIONS

The main biomass precursors are generally associated in the carbon metabolism with glycolytic activities and the tricarboxylic acids (TCA) pathway, which are diverted during recombinant protein production, causing metabolic imbalance in protein producing bacterial cells. The redox equilibrium and carbon flux diversion can be further enhanced by genomic modifications directed to the central carbon metabolism. However, the two modifications can complement each other in terms of rebalancing the redox equilibrium with carefully selected heterologous genes.

Our study subjects were genetically modified *E. coli* strains in various stages of genetic modifications designed to produce BDO; the production strain being a metabolically optimized double mutant derived from *E. coli* MG1655 harboring a two-gene heterologous biosynthetic pathway.

Taken in consideration the above, we considered essential to investigate cell behavior in case of multiple genetic modifications in our strains. Consequently, we tried to focus on the extent of adverse effects (physiological stresses) of gene deletions and heterologous genes on biomass production and strain fitness. We investigated protein production potential as well as the growth profiles of the original, gene deleted and heterologous pathway-bearing *E. coli* strains. We consider our experimental data obtained from the population dynamics and fitness testing of bacterial cultures under various carbon sources (glucose and glycerol) as being a good basis for process design and optimization in biosynthesis of valuable chemicals. Moreover, they provide a good starting point for further scale-up experiments and deeper physiological investigations (gene expression, transcriptomics) for such bacterial strains.

## EXPERIMENTAL SECTION

The list of bacterial strains used in this study is presented in Tab. 1.

**Table 1.** Bacterial strains, plasmids and oligonucleotides used in this study

| Strain | Relevant genotype | Purpose | Source |
|---|---|---|---|
| MG1655 | K-12 F– λ– ilvG– rfb-50 rph-1 | Original *E. coli* strain for gene deletions and *sucCD* cloning | DSMZ |
| BL21 STAR (DE3) | $F^-$ompThsdSB($r_B^-$, $m_B^-$) *galdcmrne*131(DE3) | *E. coli* strain for routine T7 expression | Novagen |
| MG1655(DE3) | | Wt strain with DE3-lysogenization | This study |
| MG14D1(DE3) | MG1655 (DE3) Δ*pflB* | Lysogenized *pflB* deletional mutant | This study |
| MG14D2(DE3) | MG1655 (DE3) Δ*pflB*Δ*ldhA* | Lysogenized *pflB*, *ldhA* double deletional mutant | This study |
| MG14D2(DE3)pC | MG1655 (DE3) Δ*pflB*Δ*ldhA* pETDuet1 | Control strain | This study |
| MG14D2(DE3)pGS2 | MG1655 (DE3) Δ*pflB*Δ*ldhA* harbouring pGS2 | Production strain | This study |
| MG14D2(DE3)pGS2.1 | MG1655(DE3) Δ*pflB*Δ*ldhA* harbouring pGS2.1 | Production strain | This study |
| *Chloroflexus aurantiacus* | WT | Strain for *mcr* cloning | DSMZ |
| *E. coli* (Top10F') | F', mcrA Δ(mrr-hsdRMS-mcrBC), recA1 araD139 galU galK rpsL endA1 nupG | Replication host | Invitrogen |

The list of plasmids and oligonucleotides is presented in Tab. 2. Coding sequences were obtained by gene-specific PCR reactions using as templates genomic DNA from *Chloroflexus aurantiacus (DSMZ)* and *E. coli* MG1655, followed by standard restriction cloning and ligation techniques (Table3).

Subcloning the sequences into pETDuet1 was performed by cleaving the vector and PCR products with restriction enzymes *EcoRI-HindIII* in case of *mcr* and with *AatI-XhoI* in case of *sucCD*, followed by isolation and purification of the bands of the vector fragments (GeneJET Gel Extraction Kit, Thermo Fisher Scientific), respectively of the insert (see digestion and ligation details of *mcr* in Table 4).

**Table 2.** Plasmids and oligonucleotides used in this study

| **Plasmid** | | | |
|---|---|---|---|
| pETDuet-1 | Ampr, lacI, T7lac | Coexpression vector | Merck - Millipore |
| pGS2 | pETDuet-1 harbouring *mcr* | Expression vector for *mcr* | This study |
| pGS2.1 | pETDuet-1 harbouring *mcr* and *sucCD* | Coexpression vector for *mcr* and *sucCD* | This study |
| **Oligonucleotide** | | | |
| *SucCD1AatIFor* | 5′gccacagacgtcatgaacttacatgaatatcag | Cloning primers for *sucCD* | |
| *SucCD1XhoIRev* | 5′cgatatctcgagtttcagaacagttttcagtgc | | |
| *Mcr1EcoRIFor* | 5’gagaattcaatgagcggaacaggacgactg | Cloning primers for *mcr* | |
| *Mcr1HindIIIRev* | 5’ccaagcttttacacggtaatcgccccgtcc | | |
| *ΔpflB3* | 5′aaatccacttaagaaggtaggtg | Verification primers for *pflB* | |
| *ΔpflB4* | 5′tcgtggagcctttattgtac | | |
| *ΔldhA3* | 5′gcacaaagcgatgatgctgtag | Verification primers for *ldhA* | |
| *ΔldhA4* | 5′ccgttcagttgaaggttgcg | | |

**Table 3.** PCR reaction for *mcr* amplification

| | | **PCR Protocol** | |
|---|---|---|---|
| Template DNA | 20 ng | Initial denaturation | 98ºC |
| HF buffer | 1× | Denaturation | 98ºC |
| Forward primer | 0.5 µM | Annealing | 63ºC |
| Reverse primer | 0.5 µM | Extension | 72ºC |
| dNTP | 200 µM each | Final extension | 72ºC |
| *Phusion* polymerase | 2 U | Hold | 4ºC |
| upH2O | | | |

Ligation was carried out with T4 DNA ligase (Thermo Fisher Scientific), thereafter the products were test digested and verified by sequencing (UDGenomed, Hungary). All buffers, restriction and ligase enzymes used were obtained from Thermo Scientific. DE3-lysogenization was applied (λDE3 Lysogenization Kit, Novagen, Merck Millipore) for expression of heterologous genes under the control of T7 promoter, according to the manufacturer’s instructions.

**Table 4.** Digestion and ligation reactions used for the pETDuet-*mcr* construct

| **Digestion with *EcoRI* + *HindIII*** | | Ligation pETDuet-*mcr* | |
|---|---|---|---|
| Template DNA | 100 ng | Digested pETDuet-1 | 1× |
| R buffer | 1× | *mcr* gene | 3× |
| *EcoRI* | 10 U | T4 buffer | 1× |
| *HindIII* | 10 U | T4 DNA ligase | 10 U |
| upH2O | | upH2O | |
| Incubation 2 hours at 37°C | | | |

Cultures for protein expression were obtained by transformation of chemically competent mutant strains by heat-shock with co-expression vectors pGS2 and pGS2.1. Transformed colonies were selected on LB plates containing 100 μg/mL ampicillin (Sigma). Starter cultures from a single colony were grown overnight at 37°C in LB medium containing 100 μg/mL ampicillin. To produce the target protein, a volume of 50 mL LB medium supplemented with 100 μg/ml ampicillin was inoculated from the starter culture to $OD_{595}$=0.05 and was grown at 37°C until $OD_{600}$=0.6. Expression was induced by isopropyl β-D-1-thiogalactopyranoside (IPTG, Sigma) in a final concentration of 0.5 mM. The culture was maintained at 37°C in a shaking incubator at 250 rpm for 3h, and samples were harvested by centrifugation (12000 rpm for 5 minutes). Separation of cellular proteins was performed by SDS-PAGE.

For growth dynamics experiments inoculum cultures were set up starting from a single colony, cells were grown in complex media (Luria-Bertoni media supplied with 50 μg/mL ampicillin) at 37°C and 160 rpm until reaching the mid-log phase. Minimal media were inoculated to an initial $OD_{595}$ of 0.1, containing as carbon source glucose or glycerol at 5 g/L, and 0.5 mM IPTG was added (M9 mineral medium, 25 mM $Na_2HPO_4$, 25 mM $KH_2PO_4$, 50 mM $NH_4Cl$, 2 mM $MgSO_4 \times 7H_2O$, 0.05 mM $FeCl_3 \times 6H_2O$, 0.02 mM $CaCl_2 \times 4H_2O$, 0.01 mM $MnCl_2$, 0.01 mM $ZnSO_4 \times 7H_2O$, 0.002 Mm $CoCl_2$, 0.002 mM $CuCl_2$, 0.002 mM $NiCl_2$, 0.002 mM $Na_2MO_4 \times 2H_2O$, 0.002 mM $H_3BO_3$). Cultivation was carried out in microtiter plates (200 μL) covered with adhesive foils as well in hermetically sealed glass bottles (50 mL). Small volume cultures in triplicates were maintained and determination of optical density at 595 nm was performed with the BMG Fluostar Optima microplate reader, at 37°C and 160 rpm shaking. Growth dynamics were investigated for 12 hours with measurements of $OD_{595}$ values in every 30 minutes.

## REFERENCES

1. T.M. Carole, J. Pellegrino, M.D. Paster, *Appl. Biochem. Biotechnol.*, **2004**, *115*, 871–885.
2. J.J, Straathof, *Chem. Rev.*, **2014**, *114*, 1871-1908**.**
3. S. Zeng*, Curr. Opin. Biotechnol.*, **2011**, *22*, 749-757.
4. P.K. Ajikumar, K. Tyo, S. Carlsen, O. Mucha, T.H. Phon, G. Stephanopoulos, *Mol. Pharm.*, **2008**, *5,* 167-190.
5. J.D. Keasling, *Science*, **2010**, *330*, 1355-1358.
6. J. Kirby, J.D. Keasling, *Annu. Rev. Plant. Biol.*, **2009**, *60*, 335–55.
7. D.K. Marcuschamer, P.K. Ajikumar, G. Stephanopoulos, *Trends Biotechnol.,* **2007**, *25,* 417-424.
8. R. Muntendam, E. Melillo, A. Ryden, O.Kayser, *Appl. Microbiol. Biotechnol.,* **2009,** *84*,1003-1019.
9. V.G. Yadav, G. Stephanopoulos, *Curr. Opin. Microbiol.*, **2010,** *13*, 371-376.
10. S. Carneiro, E.C. Ferreira, I. Rocha, *J. Biotechnol.,* **2013,** *164,* 396– 408.
11. V.G. Yadav, M.D. Mey, C.G. Lim, P.K. Ajikumar, G. Stephanopoulos, *Metab. Eng.*, **2012,** *14*, 233-241.
12. J.T. Kittleson, G.C. Wu, J.C. Anderson, Curr. Opin. *Chem. Biol.*, **2012,** *16*, 329–336.
13. M. Scott, C.W. Gunderson, E.M. Mateescu, Z. Zhang, T. Hwa, *Science*, **2010**, *330*,1099-1101.
14. H. Yim, R. Haselbeck, W. Niu, C. Pujol-Baxley, A. Burgard, J. Boldt, J. Khandurina, J.D. Travick, R.E. Osterhout, R. Stephen, J. Estadilla, S. Teisan, H.B. Schreyer, S. Andrae, T.H. Yang, S.Y. Lee, M.J. Burk, S. Van Dien, *Nat. Chem. Biol.*, **2011**, *7*, 445–452.
15. G.P. da Silva, M. Mack, J. Contiero, *Biotechnol. Adv.*, **2009**, *27*, 30-39.
16. S.S. Yazdani, R. Gonzalez, *Metab. Eng.*, **2008**, *10*, 340– 351.
17. V.F Wendisch, S.N. Lindner, T.M. Meiswinkel, *Biodiesel- Quality, Emissions and By-Products*, IntechOpen, London, **2011**, 305–339.
18. I. Miklóssy, Zs. Bodor, K.Cs. Orbán, R. Sinkler, Sz. Lányi, B. Albert, *J. Biomol. Struct. Dyn.,* **2016**, *35*, 1874-1889.
19. K.A. Datsenko, B.L. Wanner, *Proc. Natl. Acad. Sci.,* **2000***97*, 6640-6645.
20. J.F. Sambrook, D.W. Russell, *Molecular Cloning: A Laboratory Manual* 3rd ed., *Cold Spring Harbor Laboratory Press*, New York, **2001**
21. P. Zhou, Y. Zhang, P. Pixiang, J. Xie, Q. Ye, *Ann. Microbiol.*, **2014***64*, 219-227.
22. C. Gao, L. Zhang, Y. Xie, C. Hu, Y. Zhang, L. Li, Y. Wang, C. Ma, P. Xu, *Bioresour. Technol.*, **2013**137,111-115.
23. D.R. Nielsen, S.H. Yoon, C.J. Yuan, K.L.J. Prather, *Biotechnol. J.*, **2010**, *5*, 274-284.
24. W.S. Jung, J.H. Kang, H.S. Chu, I.S. Choi, K.M. Cho, *Metab. Eng.,* **2014**, *23*, 116-122.